phase of previously induced LTP [U. Frey, K. Schollmeier, K. G. Reymann, T. Seidenbecher, *Neuroscience* **67**, 799 (1995); U. Frey and R. G. M. Morris, *Nature* **385**, 533 (1997)]. The tetanic current was passed between pairs of the four poles of stimulation sites (a, b, c, and d) of the two cross-bundle stimulation electrodes (Fig. 1A, left). The choice of anode and cathode was systematically altered between tetanization episodes, subject to the constraint that anode and cathode were always on opposite sides of the angular bundle. In each episode, eight pulse trains (each consisting of eight stimuli at 400 Hz) were first passed at 2-s intervals between two of the poles (for example, a and c); 1 min later, a similar train was given at the opposite polarity. Then, after another 1-min interval, the whole sequence was repeated with the two other poles (for example, b and d). The choice of the anode and cathode pairs was as follows: ac and bd (episode 1), ad and bc (episode 2), bd and ac (episode 3), and bc and ad (episode 4). The fifth episode was a repetition of the first (ac and bd). Electroencephalogram epochs were recorded at 4-s intervals for 1 min after each tetanization (all combinations of stimulation across the bundle) in a subset of eight tetanized animals, and the samples were screened carefully for afterdischarges. Control rats (also lesioned and implanted) also received eight pulses at 2-s intervals, which were repeated twice within each stimulation episode. In both groups, the intensity was adjusted to evoke fEPSPs at 80 to 90% of the maximum obtained with these electrodes (500 to 2000 μA and 100-μs pulse width). Nonstimulated rats also received a unilateral hippocampal lesion, and 9 rats out of 14 were implanted.

14. T. J. Shors, T. B. Seib, S. Levine, R. F. Thompson, *Science* **244**, 224 (1989); L. Xu, R. Anwyl, M. J. Rowan, *Nature* **387**, 497 (1997).
15. E. Moser, I. Mathiesen, P. Andersen, *Science* **259**, 1324 (1993).
16. Four of these animals showed <10% on the test for residual LTP (*18*).
17. Behavioral testing was conducted in a water maze, a 198-cm-diameter pool with a featureless white surface, filled to a depth of 40 cm with water at 25° ± 2°C [R. G. M. Morris, *J. Neurosci. Methods* **11**, 47 (1984)]. Latex liquid was added to make the water opaque. A pneumatic escape platform (11 cm in diameter) was located at a fixed position midway between the center and the periphery of the pool. The platform could be moved vertically between an upper available position (1.5 cm below the water surface) and a lower unavailable position (22 cm below the water level) by remote control. Behavioral training started 7 hours after tetanic stimulation was completed. The rats were trained hourly in blocks of two trials, which were separated by 15 s (a total of 10 blocks, corresponding to trials 1 through 20), and were released from one out of eight equally spaced start positions along the perimeter of the pool in a pseudorandom predetermined order. If the rat failed to find the platform within 120 s, the rat was guided onto it. The rat was always left on the platform for 30 s. The position of the black head of the swimming rat was identified and stored at 10 Hz by a video tracking system (VP200, HVS Image, Hampton, UK; Watermaze Software, Edinburgh, UK). Probe tests (with the platform initially unavailable) were conducted on the first trial of blocks 1, 6, and 8 to assess the spatial precision of the search behavior. The platform was kept on the bottom of the pool for the first 40 s and then raised. A final transfer test with the platform submerged for 60 s was conducted at the end of training (called block 11, although consisting of only one trial). On probe trials during training, the latency to cross the platform location was substituted for the actual latency to climb the platform.
18. The extent of saturation at perforant-path/granule-cell synapses was estimated after the completion of the water maze training by tetanizing the fibers activated by the central electrode. The tetanization consisted of two blocks of eight 400-Hz pulses repeated eight times at 2-s intervals and at the same polarity. There was a 1-min interval between the blocks. The tetanization intensity was adjusted to evoke fEPSPs at 80 to 90% of maximum, as above. After the completion of these tests, the rats were killed with an overdose of Equithesin and perfused intracardially with saline and 4% formaldehyde. The brains were stored in formaldehyde for >1 week. Frozen sections were cut coronally (25 μm) and stained with cresyl violet, and the sections were examined for hippocampal and extrahippocampal damage. Sixteen animals (4 HF, 6 LF, and 6 NS) were excluded because of neocortical or thalamic lesions or because of incomplete hippocampal lesions. The exclusion of these animals did not change the pattern of results. Analyses conducted on the entire data set ($n = 43$) gave group [$F(2,40) = 4.3$, $P = 0.02$] and groups × block [$F(18,360) = 2.0$, $P < 0.005$] effects on escape latency and gave a groups × quadrants effect on the probe tests [$F(6,120) = 3.3$, $P < 0.005$].
19. The population spike increased 0.61 ± 0.30 mV (HF group) and 1.34 ± 0.68 mV (LF group). The increase in the HF group was not related to fEPSP enhancement.
20. This conclusion is corroborated by a pilot experiment suggesting that the disruption of spatial learning after LTP saturation is reversible. Six animals receiving HF stimulation were impaired when tested subsequently in a delayed-matching task in the water maze [R. G. M. Morris, J. J. Hagan, J. N. P. Rawlins, *Q. J. Exp. Psychol.* **38B**, 365 (1986)]. These animals showed no improvement in escape latency from the first to the second trial (trial 2 latencies were, on average, 6.5 s longer; there was an intertrial interval of 2 hours). One month later, when LTP had decayed, the animals showed clear evidence of learning from trial 1 to trial 2 on the same test. Latencies were 20.9 s shorter in trial 2 than in trial 1. In NS control rats, the difference was 34.0 s.
21. M. F. Yeckel and T. W. Berger, *J. Neurosci.* **18**, 438 (1998).
22. M. Nosten-Bertrand *et al.*, *Nature* **379**, 826 (1996).
23. M. L. Errington, T. V. P. Bliss, R. J. Morris, S. Laroche, S. Davis, *ibid.* **387**, 666 (1997).
24. D. Marr, *Proc. R. Soc. London Ser. B* **262**, 23 (1971); A. Treves and E. T. Rolls, *Hippocampus* **4**, 374 (1994).
25. R. G. M. Morris, E. Anderson, G. S. Lynch, M. Baudry, *Nature* **319**, 774 (1986); A. J. Silva, R. Paylor, J. M. Wehner, S. Tonegawa, *Science* **257**, 206 (1992); J. Z. Tsien, P. T. Huerta, S. Tonegawa, *Cell* **87**, 1327 (1996).
26. We thank P. Andersen for helpful advice and R. Pedersen, P. Spooner, A.-K. Amundgård, K. Haugen, K. Barmen, and G. Dyb for technical assistance. This work was supported by grants from the Human Frontiers Science Panel, the British Medical Research Council, NSF, and the Norwegian Research Council.

28 May 1998; accepted 4 August 1998

Protein Kinase C Isotypes Controlled by Phosphoinositide 3-Kinase Through the Protein Kinase PDK1

J. Ann Le Good,* Wolfgang H. Ziegler,* Davey B. Parekh, Dario R. Alessi, Philip Cohen, Peter J. Parker†

Phosphorylation sites in members of the protein kinase A (PKA), PKG, and PKC kinase subfamily are conserved. Thus, the PKB kinase PDK1 may be responsible for the phosphorylation of PKC isotypes. PDK1 phosphorylated the activation loop sites of PKCζ and PKCδ in vitro and in a phosphoinositide 3-kinase (PI 3-kinase)–dependent manner in vivo in human embryonic kidney (293) cells. All members of the PKC family tested formed complexes with PDK1. PDK1-dependent phosphorylation of PKCδ in vitro was stimulated by combined PKC and PDK1 activators. The activation loop phosphorylation of PKCδ in response to serum stimulation of cells was PI 3-kinase–dependent and was enhanced by PDK1 coexpression.

Many protein kinases require phosphorylation within their activation loops in order to express full catalytic potential. Such activation loop phosphorylations are also important for protein kinases regulated acutely by allosteric effectors. This is exemplified by PKC, where the Ca^{2+}/diacylglycerol (DAG)–dependent isotypes PKCα and PKCβ display an absolute requirement for phosphorylation in their respective activation loops (*1*, *2*). PKC has been implicated in the control of many cellular processes through the action of the second messenger diacylglycerol and as a receptor for the phorbol ester class of tumor promoters (*3*). There is overlapping specificity for one upstream kinase activity acting on the COOH-terminal hydrophobic sites in PKCα and δ and the equivalent site in PKB (*4*). To assess whether this was also the case for the conserved activation loop sites of PKC and PKB, we tested whether the PKB activation loop kinase PDK1 phosphorylated recombinant PKC.

PKCζ was phosphorylated by recombinant PDK1 (Fig. 1A); incorporation greatly exceeded the basal autophosphorylation of PKCζ itself. The maximum stoichiometry of phosphorylation observed was 2 mol/mol (as deter-

J. A. Le Good, W. H. Ziegler, D. B. Parekh, P. J. Parker, Protein Phosphorylation Laboratory, Imperial Cancer Research Fund, 44 Lincoln's Inn Fields, London WC2A 3PX, UK. D. R. Alessi, and P. Cohen, Department of Biochemistry, Medical Sciences Institute, Dundee University, Dundee DD1 4HN, UK.

*These authors contributed equally to this work.
†To whom correspondence should be addressed.

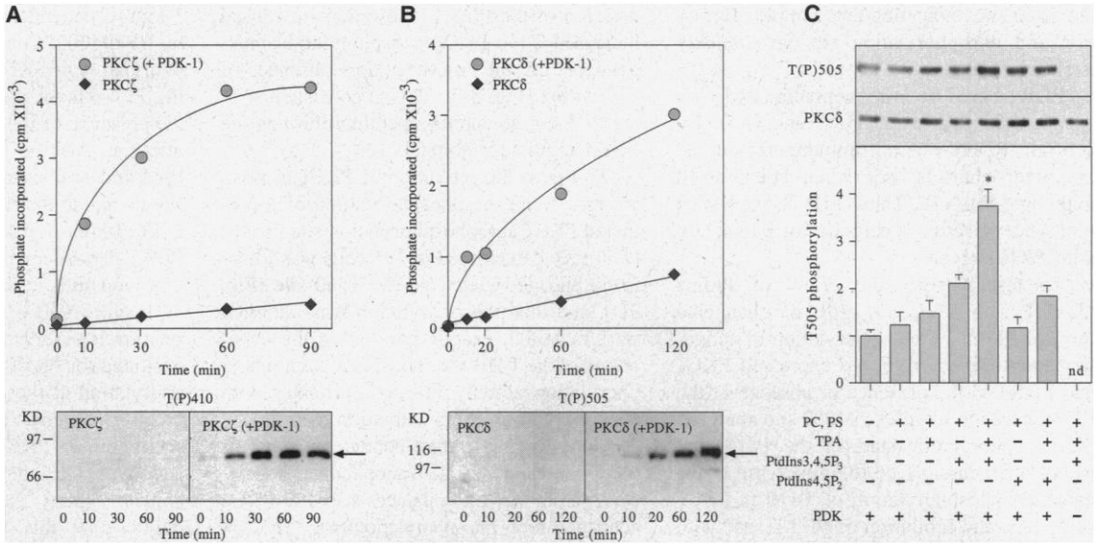

Fig. 1. Phosphorylation of PKCζ and PKCδ by PDK1 in vitro. PKCζ (**A**) and PKCδ (**B** and **C**) were phosphorylated in vitro with purified PDK1. Incorporation of ^{32}P-orthophosphate (graphs) and immunoreaction with antisera specific for phosphorylated epitopes are shown. In (C), phosphorylation of PKCδ (1 hour) was detected with antiserum T(P)505 (*20*) and is quantified (n = 3 to 6) as a function of PKCδ protein. PKCζ was purified from insect cells essentially as described (*21*). PKCδ was expressed as an NH_2-terminal glutathione S-transferase fusion protein in bacteria and purified as instructed by the manufacturer (Pharmacia). PDK1 was purified from 293 cells as described (*16*). Incubations were carried out in the presence of phosphatidylserine (PS; 100 μM), PtdIns(3,4,5)P_3 (10 μM), phosphatidylcholine (PC; 100 μM), and TPA (0.5 μM) (A and B) or with PtdIns(4,5)P_2 (10 μM) as indicated in (C); lipids were prepared as described (*22*). The combined effect of PtdIns(3,4,5)P_3 and TPA produced a significant stimulation of PKCδ phosphorylation (analysis of variance; $P < 0.02$, n = 4).

mined by ^{32}P-orthophosphate incorporation), contributed both by PDK1 and autophosphorylation. A site-specific antiserum, T(P)410, that selectively recognizes PKCζ phosphorylated on Thr^{410} (T410) bound to PKCζ phosphorylated by PDK1. PKCδ was also a substrate for PDK1 (Fig. 1B). For PKCδ the maximum stoichiometry of phosphorylation obtained was 0.5 mol/mol. PKCδ was also phosphorylated in the activation loop site (T505) as measured with a site-specific antiserum, T(P)505.

PKCδ undergoes allosteric activation by TPA (12-*O*-tetradecanoylphorbol 13-acetate) or DAG in the presence of phosphatidylserine, and PDK1 displays dependence on phosphatidylinositol 3,4,5-trisphosphate [PtdIns(3,4,5)P_3]. To determine the effects of lipids on the phosphorylation of PKCδ by PDK1, we tested various combinations of TPA, phosphatidylserine, PtdIns(3,4,5)P_3, and phosphatidylcholine. Only the combination of TPA and PtdIns(3,4,5)P_3 in the presence of the other lipids produced a significant (3.7-fold) stimulation in the rate of PKCδ phosphorylation by PDK1 ($P < 0.02$; n = 4). This effect was specific for PtdIns(3,4,5)P_3 with no stimulation by PtdIns(4,5)P_2. PKCζ is not stimulated by TPA or DAG and no effect of these lipids was observed (*5*).

PKCζ phosphorylation of a pseudosubstrate peptide (*6*) was increased up to sixfold after phosphorylation by PDK1. This degree of activation is not maximal, because the stoichiometry of T410 phosphorylation was less than 1 mol/mol. PKCδ was also activated, but transiently, due to the instability of the bacterially expressed protein. Brief incubations with PDK1 (stoichiometry of phosphorylation <0.2 mol/mol) increased PKCδ activity (*7*) approximately twofold.

To assess the interaction of PDK1 and PKC in vivo, we coexpressed the proteins in 293 cells. Immunoprecipitation of PKCζ and protein immunoblotting demonstrated that PDK1 was associated with PKCζ (Fig. 2A). Conversely, PKCζ was immunoprecipitated with PDK1 (Fig. 2B). Complex formation between PKCζ and PDK1 required the PKCζ kinase domain, and this was sufficient to mediate the interaction (Fig. 2A). Deletions within the PDK1 cDNA revealed that the kinase domain of this protein is also sufficient for complex formation with PKCζ (Fig. 2B). A proportion of the PKCζ immunoprecipitated with PDK1 was phosphorylated on

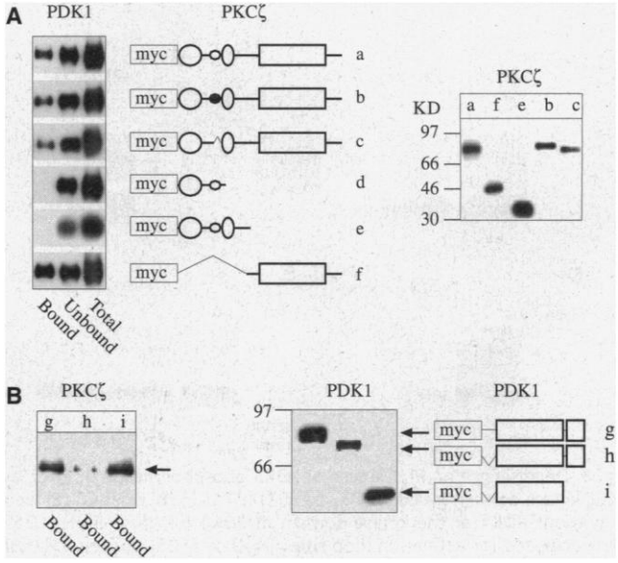

Fig. 2. PKC binding to PDK1 in 293 cells. (**A**) (Left) Myc epitope–tagged PKCζ constructs and PDK1 were expressed in 293 cells. PKCζ was immunoprecipitated, and bound, unbound, and total PDK1 were detected by immunoblotting the same cell equivalents. Myc-tagged full-length (construct a), pseudosubstrate A119E mutant (construct b), pseudosubstrate deletion (Δ116–122; construct c), V0 domain [amino acids (aa) 1 to 135] (construct d), regulatory domain (aa 1 to 232) (construct e), and kinase domain (aa 232 to 595) (construct f) PKCζ constructs were all tested for complex formation as indicated. (Right) The amounts of expressed proteins are indicated; these immunoblots were carried out on the immunoprecipitated samples shown in the left panel. Plasmid construction and transfections were carried out as described (*23*); immunoprecipitations and immunoblots were carried out as described (*24*). (**B**) (Left) Myc-tagged full-length PDK1 (construct g), PDK1 (aa 51 to 556) (construct h), and PDK1 (aa 51 to 404) (construct i) were cotransfected with full-length PKCζ and the PDK1 immunoprecipitated. Coprecipitated PKCζ was detected by immunoblot. (Right) The expression levels of the PDK1 deletion mutants were determined from the immunoprecipitates by immunoblot.

the T410 site, indicating that complex formation and phosphorylation are not mutually exclusive (*8*).

PDK1 could be immunoprecipitated with coexpressed PKCα, β_1, δ, ε, and i (*5*). By contrast, PDK1 was not immunoprecipitated in vector controls, nor when coexpressed with myc-Raf (*5*). Thus, PDK1 displays a broad but selective specificity for interaction with PKC isotypes.

To test whether the effect of PtdIns $(3,4,5)P_3$ on PKC (*9*, *10*) is channeled through PDK1 by phosphorylation of activation loop sites in vivo, we expressed PKCζ and PDK1 in the presence or absence of the PI 3-kinase inhibitor LY294002 and analyzed the phosphorylation state of the T410 site. PDK1 coexpression led to an increase in the extent of phosphorylation of T410 in PKCζ (Fig. 3A), and inhibition of PI 3-kinase with LY294002 reduced this accumulation of T410-phosphorylated PKCζ. Furthermore, the endogenous kinase that phosphorylates PKCζ T410 is also sensitive to PI 3-kinase inhibition (Fig. 3A, long). Thus, there appears to be a PI 3-kinase–dependent step in the PDK1 phosphorylation of PKCζ. To investigate whether the PI 3-kinase dependence was directed at PDK1, PKCζ, or both, we determined the LY294002 sensitivity of the phosphorylation of a kinase domain fragment of PKCζ (Δ1-232PKCζ). On coexpression of PDK1 with PKCζ (Δ1-232), the phosphorylation of the T410 site increased. As observed for wild-type PKCζ, this response was sensitive to LY294002 (Fig. 3B). Conversely, expression of the PDK1 kinase domain caused increased T410 PKCζ phosphorylation independent of the presence or absence of LY294002 (Fig. 3C). This is consistent with the PI 3-kinase control operating through the PDK1 regulatory domain.

To assess the activation of PKCζ in vivo, we monitored the phosphorylation of a predicted PKCζ autophosphorylation site (T560) (*11*). PKCζ expressed in 293 cells was found to be phosphorylated on the T560 site (Fig. 3D), and this phosphorylation was inhibited by LY294002, exactly paralleling the occupation of the T410 site. Thus, PKCζ autophosphorylation activity in vivo correlates with phosphorylation in its activation loop site.

Under normal culture conditions, PKCδ is phosphorylated in its activation loop site. However, serum starvation induces a loss of PKCδ activation loop phosphorylation (Fig. 3E). On restimulation with serum, PKCδ is acutely phosphorylated at this site by an endogenous protein kinase and LY294002 inhibits this phosphorylation. The serum-stimulated phosphorylation is enhanced by coexpression of PDK1 and this response is also LY294002-sensitive (Fig. 3E). Thus, PKCδ displays a serum-induced phosphorylation of its activation loop site that is dependent on a PI 3-kinase input and increased by PDK1 coexpression.

The results demonstrate that PKCδ and ζ are subject to control by PDK1. This is evidenced in vitro with purified proteins as well as in vivo through analysis of activation loop phosphorylation states and the influence of coexpressed PDK1. The effect of PDK1 is PI 3-kinase–dependent, being inhibited in vivo by LY294002. Consistent with this, the phosphorylation of PKCδ in vitro is stimulated by the PI 3-kinase product, PtdIns$(3,4,5)P_3$, in the presence of the PKC activator TPA. This effect is specific for the 3-phosphorylated lipid and is not supported by PtdIns$(4,5)P_2$. We conclude that PKC is controlled through a PI 3-kinase pathway, operating through PDK1-dependent phosphorylation of activation loop sites in the PKC isotypes.

In vitro PKCα activation loop phosphorylation is essential for activity (*2*), as demonstrated for PKCβ (*1*). Suppression of phosphorylation at these PKC sites in vivo with broad-specificity dominant negative constructs blocks PKC signaling (*12*) and correlates with the induction of apoptosis in certain cell types (*13*), demonstrating the essential role of this phosphorylation in vivo. However, the mechanisms effecting this control remain unknown. Our results indicate a role for PDK1. PKCζ is shown to complex with coexpressed PDK1 in vivo, indicative of a physiological role in PKCζ control. Complex formation with PDK1 is conserved for all members of the PKC family tested (classical, novel, and atypical isotypes), but not for cRaf-1. This indicates a general control of the PKC family by PDK1 or a PDK1-related kinase (*14*). Consistent with a physiological role for PDK1, phosphorylation of both PKCζ and δ by the endogenous activation loop site kinase is sensitive to LY294002.

Activation loop phosphorylation of PKCδ and ζ by PDK1 in vitro leads to increased activity; in vivo, increased autophosphorylation of PKCζ correlates with activation loop site phosphorylation. Thus, PDK1 controls the catalytic capacity of these PKC isotypes. However, at least for PKCδ, it does not bypass the requirement for allosteric activation. The control is a priming device that increases the signal strength. Results with bacterially expressed PKCδ and an activation loop (T505A) mutant indicated that phosphorylation in the activation loop site was not required for activity (*15*). We find that bacterially expressed PKCδ has less than one-tenth the activity of the protein expressed in COS-7 cells. After PDK1 phosphorylation, the activity of bacterially expressed PKCδ may be comparable to that obtained from eukaryotes.

PDK1 and its relatives regulate multiple kinases, including PKB (*14*, *16*), $p70^{s6kinase}$ (*17*, *18*), and, as shown here, various PKC isotypes. Although PDK1 may have a conserved physiological requirement for its own activator PtdIns$(3,4,5)P_3$, for the optimum phosphorylation of PKCδ, we show that the PKC activator TPA is required. We conclude that the specificity of PDK1 action on its downstream kinase targets is afforded by the particular activators and membrane recruitment devices that interact with those targets.

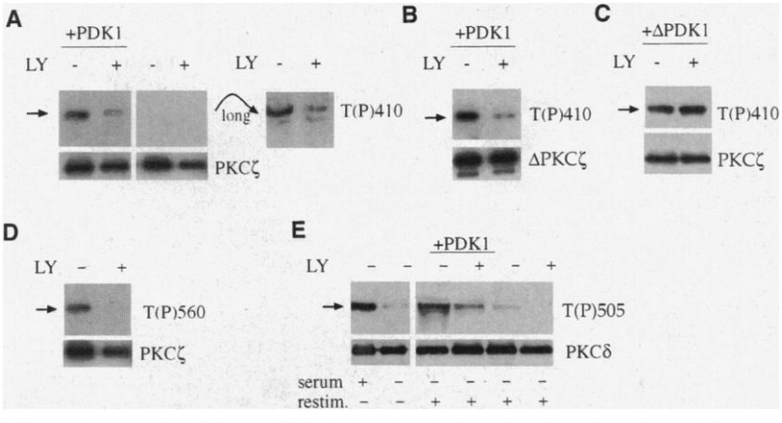

Fig. 3. Dependence on PI 3-kinase of PDK1 phosphorylation of PKCζ and PKCδ. PKCζ (**A**, **C**, and **D**), PKCζ kinase domain (residues 233 to 592) (ΔPKCζ) (**B**),or PKCδ (**E**) were expressed in 293 cells with or without PDK1 or the kinase domain of PDK1 (residues 51 to 404) (ΔPDK1). The PKC isotypes were analyzed for activation loop site (T410 or T505) phosphorylation as indicated. For PKCζ, the autophosphorylation site at T560 was also assessed through use of the site-specific T(P)560 antiserum (D). Cells were serum starved for 24 hours and treated initially with 10 μM LY294002 for 1 hour or left untreated as shown. For PKCδ-transfected cells, serum maintenance (+) or starvation (−) and restimulation (restim.) was as indicated (E). PKCζ was extracted in lysis buffer (*25*) before addition of sample buffer (*26*) for immunoblotting. PKCδ extracts were prepared directly in sample buffer. Controls for protein loading are shown. For PKCζ in the absence of PDK1, a long exposure (long) was required to detect activation loop phosphorylation (A, right). Data were quantified from scanned images. LY294002 treatment for 1 hour inhibited PDK1 phosphorylation of PKCζ and ΔPKCζ by 47 and 65%, respectively; the endogenous T410 kinase was inhibited by 53%. This is one of five similar experiments.

Direct evidence for this is provided by the finding that serum stimulation of quiescent cells induces the phosphorylation of PKCδ (Fig. 3), but not of PKCζ (*8*); this parallels the mitogen responsiveness defined by membrane association (*19*).

PKC isotypes are regulated by allosteric activation. The demonstration here that like cPKCs, both nPKCs and aPKCs are subject to phosphorylation in their activation loop sites, establishes an additional level of physiological control. The definition of the PI 3-kinase/PDK1 pathway leading to this phosphorylation would account for the role of a PI 3-kinase pathway in triggering n/aPKC-dependent responses (*9*, *10*). This pathway may thus operate in concert with the allosteric input to control PKC.

References and Notes

1. J. W. Orr and A. C. Newton, *J. Biol. Chem.* **269**, 27715 (1994).
2. S. Cazaubon, F. Bornancin, P. J. Parker, *Biochem. J.* **301**, 443 (1994).
3. H. Hug and T. F. Sarre, *ibid.* **291**, 329 (1993).
4. W. H. Ziegler *et al.*, in preparation.
5. J. A. Le Good *et al.*, data not shown.
6. N. T. Goode and P. J. Parker, *FEBS Lett.* **340**, 145 (1994).
7. A. R. Olivier and P. J. Parker, *Eur. J. Biochem.* **200**, 805 (1991).
8. J. A. Le Good, W. H. Ziegler, P. J. Parker, unpublished results.
9. K. Akimoto *et al.*, *EMBO J.* **15**, 788 (1996).
10. S. Moriya *et al.*, *Proc. Natl. Acad. Sci. U.S.A.* **93**, 151 (1996).
11. A. J. Flint, R. D. Paladini, D. E. Koshland Jr., *Science* **249**, 408 (1990).
12. P. Garcia-Paramio, Y. Cabrerizo, F. Bornancin, P. J. Parker, *Biochem. J.* **333**, 631 (1998).
13. D. H. Whelan and P. J. Parker, *Oncogene*, in press.
14. L. Stephens *et al.*, *Science* **279**, 710 (1998).
15. L. Stempka *et al.*, *J. Biol. Chem.* **272**, 6805 (1997).
16. D. R. Alessi *et al.*, *Curr. Biol.* **7**, 776 (1997).
17. D. R. Alessi, M. T. Kozlowski, Q. P. Weng, N. Morrice, J. Avruch, *ibid.* **8**, 69 (1998).
18. N. Pullen *et al.*, *Science* **279**, 707 (1998).
19. A. R. Olivier and P. J. Parker, *J. Biol. Chem.* **269**, 2758 (1994).
20. Phosphorylation site-specific antisera were generated with oligopeptides seven residues long encompassing the phosphoamino acid at residue 4. The peptides were coupled to keyhole limpet hemocyanin and used to immunize rabbits. Sera were characterized for specificity with dephospho- and phospho- forms of the peptide antigen. Protein immunoblotting analysis was carried out in the presence of dephosphopeptide (1 μg/ml) to suppress immunodetection of the dephosphorylated proteins.
21. S. Stabel, D. Schaap, P. J. Parker, *Methods Enzymol.* **200**, 670 (1991).
22. D. R. Alessi *et al.*, *Curr. Biol.* **7**, 261 (1997).
23. T. Maniatis, J. Sambrook, E. F. Fritsch, *Molecular Cloning, a Laboratory Manual* (Cold Spring Harbor Laboratory, Cold Spring Harbor, NY, 1989).
24. G. Hansra, F. Bornancin, R. Whelan, B. A. Hemmings, P. J. Parker, *J. Biol. Chem.* **271**, 32785 (1996).
25. Lysis buffer: 1% (v/v) Triton X-100, 20 mM tris-HCl (pH 7.5), leupeptin (50 μg/ml), aprotinin (50 μg/ml), 1 mM dithiothreitol, and 0.1 mM phenylmethylsulfonyl fluoride.
26. U. K. Laemmli, *Nature* **227**, 680 (1970).

27. We thank R. Marais (ICR, London) for providing the myc-pEFlink vector. We are grateful to the Deutsche Forschungsgemeinschaft (W.H.Z.), to the Medical Research Council (P.C. and D.R.A.), and to The Royal Society (P.C.) for support of this work.

7 April 1998; accepted 17 August 1998

Metapopulation Dynamics, Abundance, and Distribution in a Microecosystem

A. Gonzalez,* J. H. Lawton, F. S. Gilbert, T. M. Blackburn, I. Evans-Freke

The experimental fragmentation of landscapes of a natural ecosystem resulted in declines in the abundance and distribution of most species in the multispecies animal community inhabiting the landscapes and the extinction of many species. These declines caused the deterioration of the positive interspecific relation between local population abundance and distributional extent in this community. However, when patches were connected by habitat corridors, an immigration "rescue effect" arrested declines in both abundance and distribution and maintained the observed positive relation between them. These results demonstrate the importance of metapopulation dynamics and landscape connectivity for the persistence of populations in fragmented landscapes.

The observation that locally abundant species tend to be widespread, whereas locally rare species tend to be narrowly distributed, is one of the most pervasive patterns in ecology (*1–3*). At present, there are at least eight explanatory hypotheses, ranging from niche breadth (*4*) to sampling artifact (*5*), but each lacks conclusive evidence (*3*, *6*). A positive abundance-distribution relation is a prediction of metapopulation theory (*1*, *3*, *7–9*). One formulation of this theory, the rescue effect hypothesis (*8*), assumes that immigration decreases the probability of a local population becoming extinct (the "rescue effect") and that the rate of immigration per patch increases as the proportion of patches that are occupied increases. This rescue effect results in a positive relation between local abundance and one measure of distribution, namely the number of occupied patches. An important, but hitherto experimentally untested, consequence of this mechanism is that a reduction in the distributional extent of a species, for example, by habitat destruction, will result in a lower per patch immigration rate and thus a decline in the species' local abundance in remaining unaltered patches (*10*). A further prediction is that reduction or elimination of immigration between habitat patches inhibits the rescue effect and should result in declines in both abundance and occupancy in patches. We tested the rescue effect hypothesis for an entire animal community using a miniature, moss-based ecosystem. Moss landscapes are ideal because they are easy to manipulate in the field at a scale that is large relative to the size and dispersal abilities of the animal populations that live in them and because they contain an easily sampled, well-known, diverse community of microarthropods living at high densities (*11*). To date, experimental tests of extinction and immigration processes have been predominantly laboratory-based (*12*).

The first experiment (*13*) (Fig. 1A) examined the effects of habitat fragmentation on the distribution and abundance of species in the moss fauna. One year from the start of this experiment, species in nonfragmented control patches exhibited a strong abundance-distribution relation (Fig. 1B). However, in identically sized samples, there was a significant difference in the species richness of control and fragmented communities (*14*) [means of 17.0 ± 1.03 versus 10.3 ± 0.66 (±SEM); $F(1,11) = 27.9$, $P < 0.001$], a decline in mean species richness per patch of 40%. Surviving species still showed a positive relation between abundance and distribution in the fragments (Fig. 1C), but, as predicted by theory (*7*, *8*, *10*), the average patch occupancy and abundance of these species had both declined significantly (paired t tests: patch occupancy, $t = 8.43$, df = 20, $P < 0.001$; $\log_{10}$ abundance, $t = 4.09$, df = 20, $P < 0.001$; Fig. 1D). This experiment demonstrates how large-scale fragmentation of a landscape can result in a near universal decline in both the distribution and the abundance of the species inhabiting that landscape; even species surviving in the fragments declined in abundance,

A. Gonzalez, J. H. Lawton, T. M. Blackburn, National Environment Research Council Centre for Population Biology, Silwood Park, Ascot, Berkshire, SL5 7PY, UK. F. S. Gilbert and I. Evans-Freke, School of Biological Sciences, University Park, Nottingham University, Nottingham NG7 2RD, UK.

*To whom correspondence should be addressed. E-mail: a.gonzalez@ic.ac.uk